THE JOURNAL OF PHYSICAL CHEMISTRY B

Article

pubs.acs.org/JPCB

Stopped-Flow Kinetic Studies of Poly(amidoamine) Dendrimer–Calf Thymus DNA To Form Dendriplexes

Debabrata Dey,[†] Santosh Kumar,[‡] Souvik Maiti,[‡] and Dibakar Dhara*[,†]

[†]Department of Chemistry, Indian Institute of Technology Kharagpur, West Bengal 721302 India

[‡]Proteomics and Structural Biology Unit, Institute of Genomics and Integrative Biology, CSIR, Mall Road, Delhi 110007, India

ABSTRACT: Poly(amidoamine) (PAMAM) dendrimers are known to be highly efficient nonviral carriers in gene delivery. Dendrimer-mediated transfection is known to be a function of the dendrimer to DNA charge ratio as well as the size of the dendrimer. In the present study, the binding kinetics of four PAMAM dendrimers (G1, G2, G3, and G4) with calf thymus DNA (*CT*-DNA) has been studied using stopped-flow fluorescence spectroscopy. The effect of dendrimer-to-DNA charge ratio and dendrimer generation on the binding kinetics was investigated. In most cases, the results of dendrimer–*CT*-DNA binding can be explained by a two-step reaction mechanism: a rapid electrostatic binding between the dendrimer and DNA, followed by a conformational change of the dendrimer–DNA complex that ultimately leads to DNA condensation. It was observed that the charge ratio on the dendrimer and the DNA phosphate groups, as well as the dendrimer generation (size), has a marked effect on the kinetics of binding between the DNA and the dendrimers. The rate constant (k_1') of the first step was much higher compared to that of the second step (k_2'), and both were found to increase with an increase in dendrimer concentration. Among the four generations of dendrimers, G4 exhibited significantly faster binding kinetics compared to the three smaller generation dendrimers.

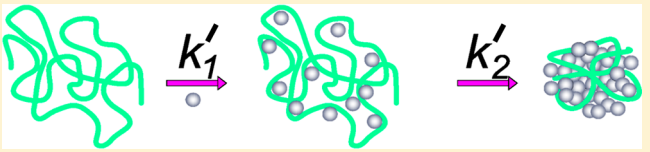

INTRODUCTION

In recent years, nonviral gene delivery has received specific attention from numerous researchers due to its advantage over in vivo viral gene delivery.[1−6] Cure of critical diseases such as inherited disorders, cancer, and AIDS may be possible in the near future by application of gene delivery techniques.[7,8] DNA–polycation complexes (polyplexes), formed as a result of electrostatic interactions between the negatively charged phosphate groups of DNA and cationic agents like multivalent cations, surfactants, lipids, polymers, and dendrimers, may be utilized for delivering nucleic acid to specific cells in the case of nonviral gene delivery.[9−11] Primary requirements for a successful gene delivery agent are (i) overall charge neutralization resulting in collapse of the DNA and polycation into a more condensed state and (ii) dissociation of DNA–polycation complexes (polyplexes) in the cytoplasm of the target cell.[7,12−14] In fact, the lifetime of the polyplexes and their dissociation in vivo play an important role in determining their efficiency. A perfect balance in the interactions between the DNA and the cationic agent is required for the polyplexes to behave as successful gene delivery agents. The size and charge of the resultant DNA–polycation complexes (polyplexes) are extremely important for facile cellular uptake of a nucleic acid via plasma membrane permeation.[15] A proper choice of cationic agent with specific architecture enables a firm control on the physiochemical characteristics, including size and charge, of the DNA–polycation complexes (polyplexes).[7,8]

Dendrimers are unique synthetic macromolecules of nanometer dimensions with a highly branched structure and globular shape.[16−19] Dendrimers serve as excellent tools for gene delivery because they form stable complexes with DNA (dendriplexes) and protect them from degradation by nucleases.[20−24] Among dendrimers, polyamidoamine (PAMAM) forms dendriplexes with nucleic acids through ionic interaction between the negatively charged backbone phosphate groups and positively charged (protonated) amino groups of polymers at physiological conditions. The interactions between PAMAM dendrimers of various generations with DNA have been studied previously.[25−27] However, the complexity of the process has prevented researchers from understanding the exact mechanism of the compaction/decompaction process of the DNA.[28] Therefore, we aimed at investigating the kinetic parameters that control the compaction process of DNA in the presence of dendrimers and the manner in which these kinetic parameters behave with increasing complexity of the dendrimer architectures. This information is extremely vital in connection to gene transport due to the fact the release kinetics of DNA from the vectors has a profound implication in gene delivery.

Previously, techniques like stopped-flow fluorescence,[29] circular dichroism,[30] and potentiometry[31] have been used to monitor the kinetics of several DNA–surfactant systems. For kinetic studies of fast reactions, where rapid mixing of reactant solutions is necessary, a stopped-flow technique has been the most widely accepted method in analytical biochemistry.[32,33] It allows two reactant solutions to be mixed rapidly and

Received: July 15, 2013
Revised: September 19, 2013

dx.doi.org/10.1021/jp406973t | *J. Phys. Chem. B* XXXX, XXX, XXX–XXX

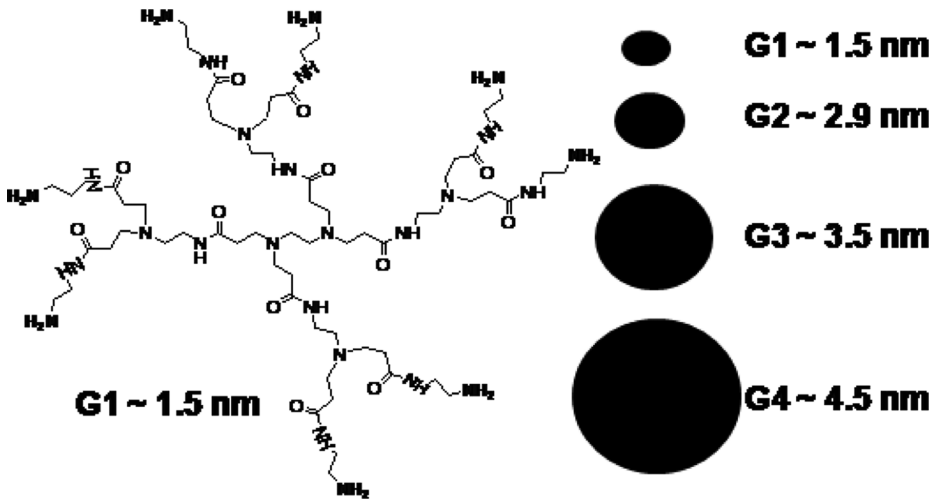

Figure 1. Chemical structure of G1 dendrimer with eight primary amine groups on the surface. A series of spheres indicating relative size of different generations of PAMAM dendrimers used in the present work.

automatically as well as measurements to be made instantaneously after mixing.[34] The fast response of the stopped-flow apparatus ensures an experimental time window in the millisecond range. This in turn helps equilibrium reactions to be studied even in those cases where one or more of the reactant species have very short lifetime in the reaction medium.[35] Owing to a better time resolution and inherent sensitivity to fast processes, fluorescence spectroscopy has been generally used to monitor stopped-flow reactions. In the present investigation, we have used stopped-flow fluorescence technique to study the kinetics of the interaction of *CT*-DNA with four generations of PAMAM dendrimers, namely, G1, G2, G3, and G4. Besides the effect of architectural complexity of dendrimers, we have also studied the effect of the DNA−dendrimer charge ratio on the kinetics of complexation.

MATERIALS AND METHODS

Materials. Sodium salt of *CT*-DNA, PAMAM dendrimers of four generations, namely, G1, G2, G3, and G4, were purchased from Sigma-Aldrich and used as received. It may be noted that *CT*-DNA supplied by Sigma-Aldrich is reported to be highly polydisperse in nature (M_w = 8 418 000 and polydispersity index = 5.2 approximately).[36] Chemical structure of one of the representative dendrimers, G1, is shown in Figure 1 along with a schematic presentation of the comparative sizes of the four dendrimers used in this work. These dendrimers can be named appropriately following the shorthand nomenclature introduced by Tomalia et al.[19] Accordingly, the nomenclature for the four PAMAM dendrimers will be as follows. (i) G1: [Core: ethylenediamine]; (4→2); *dendri*-{poly(amidoamine)-$(NH_2)_8$}; (G = 1) dendrimer (ii) G2: [Core: ethylenediamine]; (4→2); *dendri*-{poly(amidoamine)-$(NH_2)_{16}$}; (G = 2) dendrimer (ii) G3: [Core: ethylenediamine]; (4→2); *dendri*-{poly(amidoamine)-$(NH_2)_{32}$}; (G = 3) dendrimer; (iv) G4: [Core: ethylenediamine]; (4→2); *dendri*-{poly(amidoamine)-$(NH_2)_{64}$}; (G = 4) dendrimer. Stock *CT*-DNA solutions were prepared by dissolving the required amount of DNA fibers in 5 mL of 10 mM potassium phosphate buffer solution (pH = 7.2) in a 15 mL vial and kept in a orbital shaker overnight at 30 °C. The concentration of DNA stock solution was measured by a Cary 100 UV−visible spectrophotometer. The concentration of *CT*-DNA (in terms of negatively charged phosphate group) was measured by its absorbance at 260 nm and molar extinction coefficient (ε) = 6600 M^{-1} cm^{-1}. The ratio of absorbance of DNA solution at 260 and 280 nm was 1.82, and the absorbance at 320 nm was negligible, confirming the absence of any protein contamination. The DNA melting temperature was measured using a Cary 100 UV−visible spectrophotometer with temperature controller and found to be 72 °C, which was in accordance with information provided by Sigma-Aldrich. The conformation of DNA in phosphate buffer solution was measured by circular dichroism (Jasco spectropolarimeter model 715) and found to be similar to that of standard DNA. Ethidium bromide (3,8-diamino-5-ethyl-6-phenylphenanthridium bromide, EB) was purchased from Sigma-Aldrich and used without further purification. The stock solution of EB was prepared by dissolving 2.2 mg in 1 mL of phosphate buffer, and the concentration was determined by using a UV−visible spectrophotometer (ε = 5600 M^{-1} cm^{-1} at 480 nm). Ethidium bromide solutions were stored in the dark at 4 °C before use. The dendrimer stock solutions (5000 μM) were prepared by dissolving a known volume of the original dendrimer solution in a required volume of potassium phosphate buffer solution. All the experiments were carried out using 10 mM potassium phosphate buffer (pH = 7.2), prepared in Milli-Q water. All other chemicals used in this study were of AR-grade purity and used as received. Unless specified otherwise, the concentrations of DNA solutions are given in molarity units in terms of negatively charged phosphate groups in the DNA backbone.

Steady-State Fluorescence Spectroscopic Studies. Steady-state fluorescence spectra were taken in a Jobin Yvon Fluorolog spectrofluorometer. The excitation wavelength was 480 nm, with the emission spectra taken from 500 to 700 nm wavelength range. The excitation slit and emission slit were fixed at 5 and 2 nm, respectively. The temperature was set at 25 °C. To make the DNA−EB complex, the DNA stock solutions and EB stock solutions were mixed (1 EB/1 bp) in the phosphate buffer and equilibrated for 10 min. To a *CT*-DNA−EB mixture (1 mL) in a quartz cuvette were added the desired amounts of dendrimer stock solutions. For each addition of dendrimer solution, the resultant mixture was equilibrated for 10 min before recording the steady-state fluorescence spectrum. Dendrimer solutions were added to the *CT*-DNA−EB mixture

dx.doi.org/10.1021/jp406973t | *J. Phys. Chem. B* XXXX, XXX, XXX−XXX

so that the charge ratio ($Z_{+/-}$, ratio of concentration of cationic charges on dendrimer to DNA phosphate groups) varies from $Z_{+/-} = 0$ to $Z_{+/-} = 9$, and no visible turbidity occurred in this entire range.

Stopped-Flow Fluorescence Spectroscopic Studies. The kinetic measurements were carried out using a SFA-20 rapid kinetics accessory (HI-Tech Scientific) in Jobin Yvon Fluorolog with a Peltier thermostat. The concentration of both DNA and ethidium bromide in the *CT*-DNA−EB complex solution was 50 μM, and four different concentrations of the dendrimer solutions were used for the stopped-flow kinetic study (i.e., 25, 50, 150, 450 μM) to obtain the charge ratio of the resultant solutions as $Z_{+/-} = 0.5$, 1, 3, and 9, respectively, upon mixing of equal volume of two solutions. The excitation and emission monochromator were set to 480 and 590 nm, respectively. During the experiment, two separate syringes of the stopped-flow were filled up with *CT*-DNA−EB complex and dendrimer solutions, and in each run, an equal volume of both solutions was injected at once into the sample chamber. The emission spectra were monitored continuously both before ($t = 0$ s) and after the injection. The dead time of the instrument was determined from the test reaction described elsewhere[37] and was found to be 5 ms for a 1:1 mixing. Suitable control experiments were performed by mixing a *CT*-DNA−EB complex solution and buffer solutions without the dendrimer. Photobleaching of the EB dye was ruled out since the fluorescence signal of the *CT*-DNA−EB complex remained unchanged with time while carrying out the control experiments.

RESULTS AND DISCUSSION

DNA−Dendrimer Complexation. Generally, high generation PAMAM dendrimers have been found to facilitate more efficient transfection than the lower generation dendrimers. Cell transfection efficiency was shown to be lower in the case of G1, G2, and G3 dendrimers and increased from G4 onward showing a maximum in the case of G6.[38,39] It was also shown that the generation number affected the microvascular extravasation of PAMAM dendrimers. Tajarobi et al.[40] studied the transepithelial transport of a series of PAMAM dendrimers (G0 to G4) across Madin-Darby canine kidney cells in vitro. It was found that the permeability of the dendrimer was the highest for PAMAM G4 and was governed by a balance between the size of the polymer and its interaction with the cells. Results suggested that the cell integrity was compromised in the presence of PAMAM G4, thus leading to high permeability. In the present work, we have investigated the kinetics of the dendrimer−*CT*-DNA binding with the objective of understanding the fundamental aspects of binding that would explain the differences in transfection efficiencies of the lower generation and the higher generation dendrimers.

The binding kinetics of PAMAM G4 dendrimer was compared to those of the lower generation dendrimers, G1, G2, and G3. We have studied the DNA−dendrimer complexation process using EB dye by varying the charge ratio ($Z_{+/-}$) of the cationically charged dendrimer and anionically charged DNA.The four different dendrimers used for the kinetic study had varying concentration of primary amine groups on the surface (positively charged under physiological pH conditions) that enabled us to understand the effect of the dendrimer architecture on the binding process. When EB intercalates between the hydrophobic base pairs of the DNA helix, the fluorescence emission increases significantly (the light switch mechanism).[29] In order to fix the concentration range suitable for kinetic measurements, we chose to study the DNA−dendrimer complexation process by steady-state fluorescence spectroscopy. The observed fluorescence spectra for G1 and G4 dendrimers are shown in Figure 2. Addition of cationic

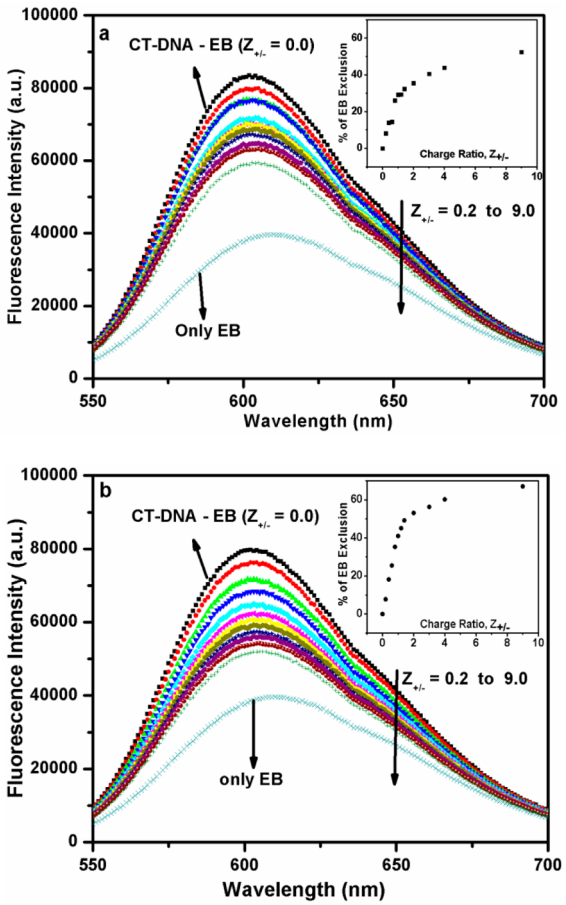

Figure 2. Ethidium bromide fluorescence spectra for (a) G1 dendrimer and (b) G4 dendrimer. Traces for fluorescence emission spectra of free EB and EB bound to *CT*-DNA are marked. The downward arrows indicate the increase of $Z_{+/-}$. The *CT*-DNA concentration was 25 μM in 10 mM phosphate buffer. In the inset, the % EB excluded is plotted against $Z_{+/-}$.

dendrimer solution in *CT*-DNA−EB complex displaces the intercalated EB molecules from the DNA helix, releasing them back into water, resulting in a decrease in the fluorescence intensity of EB. The size of the cationic dendrimer and their binding strength with DNA determined the amount of EB excluded from the DNA−EB complex. It was observed that, for a given dendrimer, the amount of EB excluded was higher with an increase in the charge ratio $Z_{+/-}$, although even at $Z_{+/-} = 9$, the EB was not totally released from DNA. It was also observed that, for a given charge ratio, G4 excluded more EB than G1, probably due to a higher surface charge density in G4 as compared to that in G1 which resulted in stronger electrostatic binding with the negatively charged *CT*-DNA. Also, partial wrapping by the DNA chains may be possible around the G4 dendrimer owing to its bigger size as compared to the smaller dendrimers,[25,41] which in turn resulted in the release of more EB from the chain into water. It is also to be noted that the DNA−EB dendrimer solutions were all optically transparent for

dx.doi.org/10.1021/jp406973t | J. Phys. Chem. B XXXX, XXX, XXX−XXX

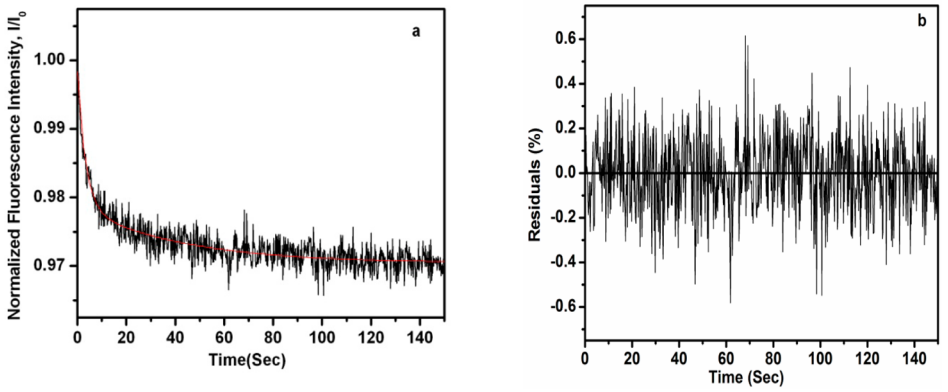

Figure 3. (a) Stopped-flow fluorescence intensity decay of G1 dendrimer−*CT*-DNA binding at $Z_{+/-}$ = 0.5, as a function of time. The smooth line shows the fitting obtained with eq 1. (b) Residuals of the fit shown in (a).

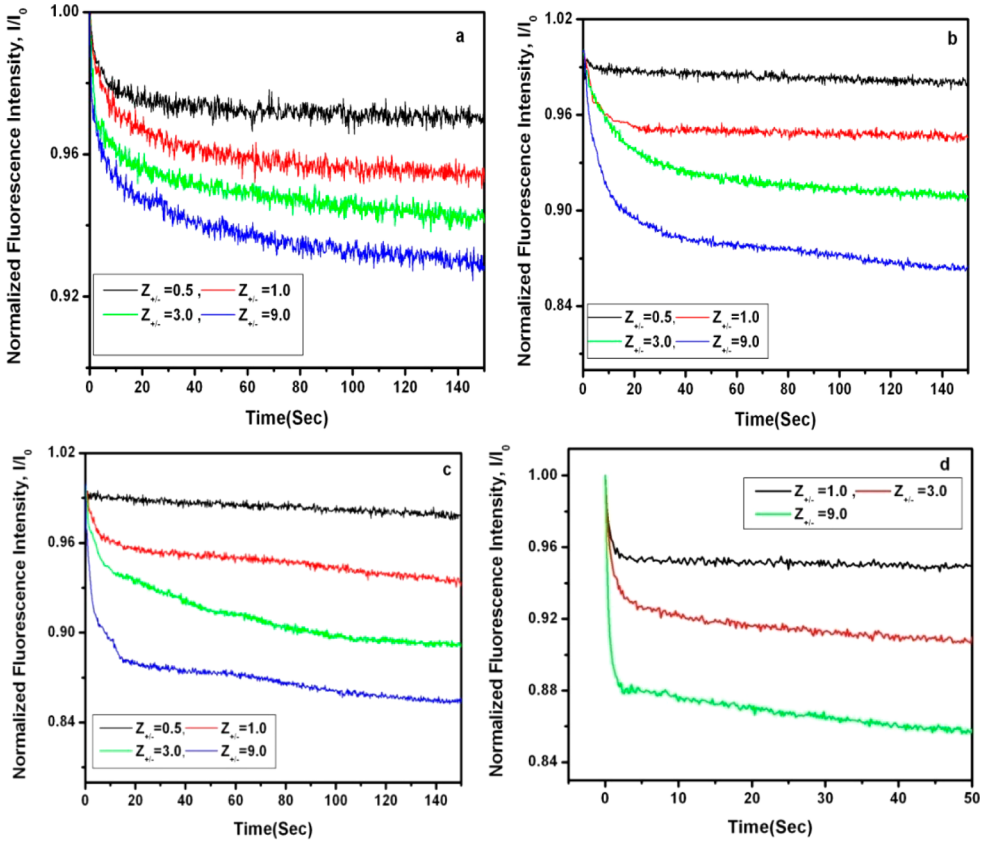

Figure 4. Fluorescence intensity of *CT*-DNA−EB complex as a function of time after mixing with PAMAM dendrimers at different dendrimer to *CT*-DNA charge ratio ($Z_{+/-}$ = 0.5, 1.0, 3.0, 9.0): (a) G1, (b) G2, (c) G3, (d) G4.

the entire range of charge ratio investigated ($Z_{+/-}$ = 0 to 9), indicating no phase separation.

Choice of Dye/DNA Ratio. In stopped-flow kinetics studies, the release of the dye is monitored rather than the direct binding of the cationic agents with DNA, and hence, the choice of the dye is also an important factor. It can be anticipated that the absolute values of the rate constants may change with variation in dye. Hence, we refer to the rate constants obtained in this study as "relative rate constants".[29,44] However, it is also comprehensible that the trends observed in the values of the relative rate constants should remain same irrespective of the dye used for the study. We have used EB as the fluorescence probe dye instead of other dyes like YOYO-1 and Hoechst 33258[30] as EB one of the most frequently used dyes for equilibrium binding studies and also for staining DNA in gel electrophoresis, and so, our kinetic data would be more relevant to most of these well-studied systems. Eastman et al.,[42] while studying the effect of cationic lipids on the DNA−EB complex, showed that the decrease of EB fluorescence with increasing lipid concentration was dependent on the EB to DNA ratio. Only when EB/DNA was larger than one EB per six nucleotides, was this decrease of EB fluorescence linearly related to the amount of cationic lipid at a given DNA concentration. At lower EB concentrations, the decrease in fluorescence showed a sigmoidal profile[43] that would lead to erroneous interpretations. To avoid this complication arising out of lower EB concentration, we have used a ratio of one EB

dx.doi.org/10.1021/jp406973t | J. Phys. Chem. B XXXX, XXX, XXX−XXX

to one nucleotide unit to ensure a linear change of the fluorescence.[44]

Data Treatment/Kinetic Analysis. The observed fluorescence kinetic curves were complex in nature, indicating the involvement of multiple steps in the complexation process. We postulated that the fluorescence decay curves are a superposition of exponential terms:

$$I(t) = \sum A_i \exp(-t/\tau_i) \quad (1)$$

where $I(t)$ is the fluorescence at time t, A_i is the prefactor, and τ_i is the pseudo-first-order time constant. The reciprocal of time constant is the rate constant k_i of the reaction. The Nelder–Mead simplex method for minimizing eq 1 was applied. The quality of the fits was assessed from the χ^2 value. Data analysis was performed using Origin 8.0 software. Kinetic data were fitted by a nonlinear least-squares method to a biexponential relationship, except for the experiments using G3 and G4 at high charge ratio ($Z_{+/-}$ = 9) that could be best fitted to a triexponential form. Figure 3a shows a typical fluorescence intensity decay of EB observed upon dendrimer (G1) binding to *CT*-DNA at $Z_{+/-}$= 0.5 in 10 mM phosphate buffer solution. The number of exponentials was increased until no systematic deviation of the residual was found (as shown in Figure 3b). Two exponentials were necessary to fit the data for this particular case.

Effect of Charge Ratio and Dendrimer Size on Binding Kinetics. In order to understand the effect of the size of the PAMAM dendrimers on the kinetics of their complexation with *CT*-DNA, it was necessary to look carefully into the dendrimer structures. All the PAMAM dendrimers have a common ethylene diamine core and an amidoamine repeat branching structure.[45,46] As the generation (G) number increases, the number of active terminal primary amine group doubles. For instance, G1 contains 8, G2 contains 16, G3 contains 32, and G4 contains 64 surface primary amine groups that become positively charged at the physiological pH conditions.[47,48] The dendrimers used here have diameter ranging from 1.5 nm (G1) to 4.5 nm (G4).[30] The lower generation dendrimers are disk-like in shape, and as the generation increases, the shape becomes more spherical in nature.[49,50] Higher generation dendrimers also have more exposed functional groups on the surface. Figure 4 shows experimental plots of fluorescence intensity as a function of time for each of the four dendrimers (G1–G4), at four different dendrimer to *CT*-DNA charge ratios ($Z_{+/-}$ = 0.5, 1.0, 3.0, 9.0) at 25 °C. The fluorescence decay curves were fitted to eq 1. Table 1 shows the reciprocal of the time constants, τ_1 and τ_2 (k_1' and k_2'), as a function of $Z_{+/-}$ for the different dendrimers at constant temperature. The rate constant values, k_1' and k_2', for the different dendrimers were also plotted against charge ratios, as shown in Figure 5. Each rate constant value (k_1' and k_2') reported here is the average of three independent experiments. The two rate constants are well-separated by at least an order of magnitude for all the dendrimers under investigation, indicating that the first step is much faster than the second. For example, k_1'/k_2' values for G2 and G4 at $Z_{+/-}$ = 1 is 24 and 210, respectively. Most of the fluorescence emission decay curves fit into the biexponential function, suggesting a two-step process, except in a few cases with higher charge ratios ($Z_{+/-}$= 9 for G3 and G4) where a three-step mechanism was found to exist.

Variation of k_1' Values. It is evident from Table 1 and Figure 5a that the k_1' values are different for different generations of dendrimers. This suggests a possible aggregation or association of the dendrimer to DNA taking place in this step since only a diffusion-driven process like binding alone cannot bring this drastic change in the relative rate constants of different generations of dendrimers. Also, association or aggregation values for different generations of dendrimers will be different and lead to differences in the observed k_1' values. A significant difference is observed in the rate constant values for different generations of dendrimers at the same charge ratio. In general, the initial rate of binding was found to be very high, and that increased with increase in $Z_{+/-}$ ratio. The first step is believed to be a completely electrostatically driven process. During the binding of negatively charged DNA and positively charged dendrimers at the physiological pH, the diffusion process plays a significant role. Therefore, in the case of a given dendrimer generation, the larger the amount of added dendrimer, the faster the reaction proceeds.

Table 1. Relative Rate Constant Values for the Different Generations of Dendrimer Binding to *CT*-DNA as a Function of Charge Ratio, $Z_{+/-}$, for a Fixed Concentration of *CT*-DNA and Temperature

dendrimer	charge ratio ($Z_{+/-}$)	$k_1' \times 10^1$ (s^{-1})	$k_2' \times 10^2$ (s^{-1})
G1	0.5	3.08 ± 0.05	2.38 ± 0.03
	1.0	3.48 ± 0.03	2.89 ± 0.07
	3.0	3.70 ± 0.08	1.50 ± 0.18
	9.0	6.84 ± 0.14	2.38 ± 0.09
G2	0.5	2.41 ± 0.09	0.83 ± 0.02
	1.0	3.18 ± 0.04	1.31 ± 0.04
	3.0	3.97 ± 0.03	1.47 ± 0.14
	9.0	11.00 ± 0.35	5.55 ± 0.22
G3	0.5	1.10 ± 0.02	0.47 ± 0.01
	1.0	2.98 ± 0.06	0.86 ± 0.03
	3.0	4.20 ± 0.05	1.57 ± 0.08
	9.0	12.13 ± 0.41	25.65[a] ± 2.13
G4	0.5	n/a[b]	n/a[b]
	1.0	14.13 ± 0.85	0.66 ± 0.02
	3.0	19.52 ± 1.46	7.19 ± 0.25
	9.0[c]	33.76 ± 2.52	108.96[c] ± 8.25

[a]Triexponential kinetic decay with appearance of a third rate constant (k_3' = 2.04 ± 0.05 × 10^{-2} s^{-1}). [b]Could not be unambiguously assigned to any of the kinetic steps. [c]Triexponential kinetic decay with appearance of a third rate constant (k_3' = 3.60 ± 0.09 × 10^{-2} s^{-1}).

Variation of k_2' Values. It is evident from Table 1 and Figure 5b that the variation of k_2' with charge ratios was quite insignificant. In this step, condensation of DNA occurred with a possible internal rearrangement of the *CT*-DNA–dendrimer complex. It has been reported that, with increasing charge ratio of dendrimers, the nature of dendrimer–DNA polyplexes becomes different.[50,51] Therefore, complexity arising due to possible internal rearrangement in the second step vastly affects the k_2' values in addition to the electrostatic binding force.

For G1 dendrimer, k_2' values remain more or less unchanged with change in $Z_{+/-}$, which indicates a weaker binding of G1 with *CT*-DNA. This is probably because the relatively smaller size of the G1 dendrimer resulted in a larger surface area and therefore a lower charge density that enabled the formation of well-structured rods and toroids.[50−52] In case of G1, as the intermediate structures during the compaction process are well-defined and not dependent on charge ratio, the variation of k_2' was insignificant with an increase in charge ratio. In the case of G2 and G3, no specific trend in k_2' values was observed with

dx.doi.org/10.1021/jp406973t | J. Phys. Chem. B XXXX, XXX, XXX–XXX

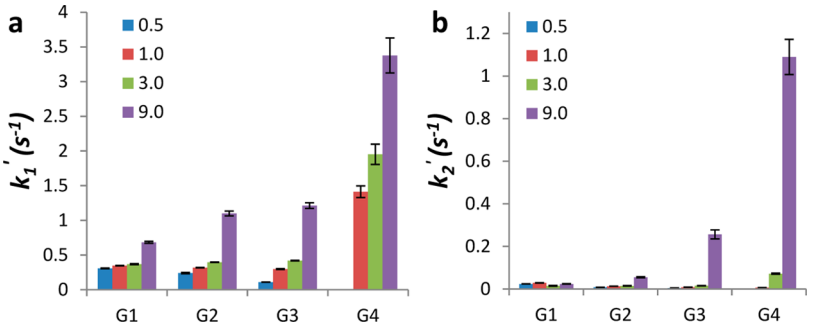

Figure 5. Relative rate constant values for the different generation of dendrimers binding to *CT*-DNA as a function of charge ratio, $Z_{+/-}$, for a fixed concentration of *CT*-DNA and temperature: (a) k_1' and (b) k_2'. The series represents the values for charge ratio.

increasing charge ratios, possibly due to formation of ill-defined intermediate structures during compaction and some other local factors. In the case of G4, a drastic increase of k_2' values was observed with increasing $Z_{+/-}$, suggesting a very strong dendrimer to DNA binding, with significant internal rearrangement occurring in the compaction process of DNA. Due to highest surface charge in the series, the G4 dendrimer is expected to stick to the oppositely charged DNA molecule on the first contact. When G4 is added to DNA, different morphologies like rods and toroids are formed, including globular ones (characteristic intermediate formed in the case of higher generation PAMAM dendrimers). This is unique for G4 in the series of PAMAM dendrimer generations investigated[50] and is supported by the drastic variation in k_2' values with increase in charge ratio $Z_{+/-}$ from 1.0 to 9. It is noteworthy that, in all cases except G1, the k_2' values were significantly higher at the charge ratio $Z_{+/-}$ = 9. Higher magnitude of k_2' might be due to possible internal arrangements of the DNA–dendrimer complex in this case governed by the thermodynamic parameters that helps in readily attaining equilibrium in the presence of excess charge of the dendrimer molecule.

In the literature, the binding kinetics of CTAB[31] and lipids[30] to DNA have been explained by a two-step mechanism. It is generally believed that complexation of DNA with a cationic agent includes (i) the electrostatic binding of positively charged groups of the cationic agent and negatively charged phosphate group of DNA. This process is relatively faster and involves potential dehydration and (ii) the condensation of DNA in the presence of oppositely charged agents. In this step, it is believed that the cationic agent aggregates in the vicinity of DNA,[44] as evident from the presence of cooperative binding[44] and existence of a liquid-crystalline phase[7,53] in these systems. The second step in which the DNA compaction occurs is relatively slower. In the present case, the binding between the dendrimers and DNA is a bimolecular process and follows a two-step mechanism. From the exponential plot, we get the two time constants of the reaction (with the exception of G3 and G4, at charge ratio $Z_{+/-}$ = 9, where a third time constant was present). Presence of more than two steps in decay kinetics at higher charge ratios for G3 and G4 indicates further rearrangement of the complex formed.

Thus, different rate constants represent different modes of binding processes. The question that may arise is that, to what extent the rate constants so obtained are dependent on the type of probe. In fact, Braun et al. have shown that different probes indeed yield differences in the rate constant values in a kinetic study, but overall trends of the rate constants are similar in nature.[30] It is well-understood that this methodology provides relative rate constants. If we choose a different fluorescent dye as the probe, then the absolute values of the rate constants may be changed because the displacement mechanisms of different dyes from the DNA double-helix are different. Again, under the present experimental conditions, the displacement mechanism of EB from DNA is expected to remain almost the same for different generations of PAMAM dendrimers. Thus, we can say that the observed differences in the relative rate constant values arise due to variations in the $Z_{+/-}$ ratios or dendrimer architecture.

CONCLUSION

The kinetic pathway of complexation reaction between *CT*-DNA and PAMAM dendrimers has been investigated by employing stopped-flow fluorescence techniques. As discussed earlier, the equilibrium studies on DNA–cationic agent bindings have been done extensively, but the kinetic pathways involving the transitions under nonequilibrium state have been much less explored. In this work, we have investigated the effect of charge ratio as well as dendrimer architecture on the kinetic parameters of dendrimer–*CT*-DNA binding. In all cases, the binding between the dendrimers and DNA is a bimolecular process and follows a two-step mechanism (with a few exceptions at $Z_{+/-}$ = 9, where a three-step path was observed), with electrostatic binding between oppositely charged DNA and dendrimer in the first step followed by conformational change of DNA in the second. Appearance of a three-step path indicates the complexity of the process brought about by existence of many intermediate forms during the course of the reaction. Electrostatic binding force is the main contributing factor in the first step, where a more spherically shaped G4 dendrimer can interact with DNA more efficiently as compared to G3, G2, and G1. Moreover, presence of a greater number of positively charged groups on the surface makes G4 dendrimers more potent to bind with the negatively charged DNA. The difference in k_2' values observed for different generations of the dendrimer are not very significant. In fact, in this step, different types of intermediate structures are formed depending upon dendrimer structure variation and charge species present in the complex,[50,51] making this step very complicated. The k_2' values in the G4 systems were found to be much higher compared to the systems with lower generation dendrimers at higher charge ratios, indicating the uniqueness of the intermediates formed during binding of G4 with DNA. This possibly correlates with the fact that G4 shows the highest gene transfection efficiency in cell lines compared to the lower generation dendrimers.

dx.doi.org/10.1021/jp406973t | J. Phys. Chem. B XXXX, XXX, XXX–XXX

AUTHOR INFORMATION

Corresponding Author

*E-mail: dibakar@chem.iitkgp.ernet.in. Phone: +91-3222-282326. Fax: +91-3222-282252.

Notes

The authors declare no competing financial interest.

ACKNOWLEDGMENTS

Financial support from the Department of Science and Technology, Government of India, New Delhi, is acknowledged. D. Dey acknowledges UGC, New Delhi, for a Senior Research Fellowship.

REFERENCES

(1) Huang, L.; Huang, M. C.; Wagner, E. *Advances in Genetics: Nonviral Vectors for Gene Therapy*, 2nd ed.; Elsevier: San Diego, CA, 2005; Vol. *53*.

(2) Niidome, T.; Huang, L. Gene Therapy Progress and Prospects: Nonviral Vectors. *Gene Ther.* **2002**, *9*, 1647−1652.

(3) Huang, L.; Huang, M. C.; Wagner, E. *Nonviral Vectors for Gene Therapy*; Academic Press: San Diego, CA, 1999.

(4) Mahato, R. I.; Kim, S. W. *Pharmaceutical Perspectives of Nucleic Acid-Based Therapeutics*; Taylor and Francis: London, 2002.

(5) Anderson, W. F. Human Gene Therapy. *Science* **1992**, *256*, 808−813.

(6) Zuber, G.; Dauty, E.; Nothisen, M.; Belguise, P.; Behr, J. P. Towards Synthetic Viruses. *Adv. Drug Delivery Rev.* **2001**, *52*, 245−253.

(7) Dias, R. S.; Lindman, B. *DNA Interactions with Polymers and Surfactants*; John Wiley & Sons: Hoboken, NJ, 2008.

(8) Mintzer, M. A.; Simanek, E. E. Nonviral Vectors for Gene Delivery. *Chem. Rev.* **2009**, *109*, 259−302.

(9) Kataoka, K.; Harada, A.; Nagasaki, Y. Block Copolymer Micelles for Drug Delivery: Design, Characterization and Biological Significance. *Adv. Drug Delivery Rev.* **2001**, *47*, 113−131.

(10) Kakizawa, Y.; Kataoka, K. Block Copolymer Micelles for Delivery of Gene and Related Compounds. *Adv. Drug Delivery Rev.* **2002**, *54*, 203−222.

(11) Braun, C. S.; Jas, G. S; Choosakoonkriang, S.; Koe, G. S.; Smith, J. G.; Middaugh, C. R. The Structure of DNA within Cationic Lipid/DNA Complexes. *Biophys. J.* **2003**, *84*, 1114−1123.

(12) Godbey, W. T.; Mikos, A. G. Recent Progress in Gene Delivery Using Non-viral Transfer Complexes. *J. Controlled Release* **2001**, *72*, 115−125.

(13) Khalil, I. A.; Kogure, K.; Akita, H.; Harashima, H. Uptake Pathways and Subsequent Intracellular Trafficking in Nonviral Gene Delivery. *Pharmacol. Rev.* **2006**, *58*, 32−45.

(14) Ilarduya, C. T. D.; Sun, Y.; Düzgünes, N. Gene Delivery by Lipoplexes and Polyplexes. *Eur. J. Pharm. Sci.* **2010**, *40*, 159−170.

(15) Kabanov, A. V. Taking Polycation Gene Delivery systems from in Vitro to in Vivo. *Pharm. Sci. Technol. Today* **1999**, *2*, 365−372.

(16) Tomalia, D. A. Birth of a New Macromolecular Architecture: Dendrimers as Quantized Building Blocks for Nanoscale Synthetic Polymer Chemistry. *Prog. Polym. Sci.* **2005**, *30*, 294−324.

(17) Tomalia, D. A. Dendrons/Dendrimers: Quantized, Nano-Element Like Building Blocks for Soft-Soft and Soft-Hard Nano-Compound Synthesis. *Soft Matter* **2010**, *6*, 456−474.

(18) Esfand, R.; Tomalia, D. A. Poly(amidoamine) (PAMAM) Dendrimers: From Biomimicry to Drug Delivery and Biomedical Applications. *Drug Discovery Today* **2001**, *6*, 427−436.

(19) Tomalia, D. A.; Christensen, J. B.; Boas, U. *Dendrimers, Dendrons and Dendritic Polymers*; Cambridge University Press: Cambridge, UK, 2012; pp 29−33.

(20) Wang, R.; Zhou, L.; Zhou, G.; Li, G.; Zhu, B.; Gu, H.; Jiang, X.; Li, H.; Wu, J.; He, L.; Guo, X.; Zhu, B.; Yan, D. Synthesis and Gene Delivery of Poly(amido amine)s with Different Branched Architecture. *Biomacromolecules* **2010**, *11*, 489−495.

(21) Fant, K.; Esbjorner, E. K.; Jenkins, A.; Grossel, M. C.; Lincoln, P.; Norden, B. Effects of PEGylation and Acetylation of PAMAM Dendrimers on DNA Binding, Cytotoxicity and in Vitro Transfection Efficiency. *Mol. Pharmaceutics* **2010**, *7*, 1734−1746.

(22) Templeton, N. S. *Gene Therapy: Therapeutic Mechanisms and Strategies*, 2nd ed.; Dekker: New York, 2004.

(23) Lee, C. C.; Mackay, J. A.; Frechet, J. M. J.; Szoka, F. C. Designing Dendrimers for Biological Applications. *Nat. Biotechnol.* **2005**, *23*, 1517−1526.

(24) Dufes, C.; Uchegbu, I. F.; Schätzlein, A. G. Dendrimers in Gene Delivery. *Adv. Drug Delivery Rev.* **2005**, *57*, 2177−2202.

(25) Chen, W.; Turro, N. J.; Tomalia, D. A. Using Ethidium Bromide To Probe the Interactions between DNA and Dendrimers. *Langmuir* **2000**, *16*, 15−19.

(26) Kabanov, V. A.; Sergeyev, V. G.; Pyshkina, O. A.; Zinchenko, A. A.; Zezin, A. B.; Joosten, J. G. H.; Brackman, J.; Yoshikawa, K. Interpolyelectrolyte Complexes Formed by DNA and Astramol Poly(propylene imine) Dendrimers. *Macromolecules* **2000**, *33*, 9587−9593.

(27) Orberg, M. L.; Schillen, K.; Nylander, T. Dynamic Light Scattering and Fluorescence Study of the Interaction between Double-Stranded DNA and Poly(amido amine) Dendrimers. *Biomacromolecules* **2007**, *8*, 1557−1563.

(28) Froehlich, E.; Mandeville, J. S.; Weinert, C. M.; Kreplak, L.; Tajmir-Riahi, H. A. Bundling and Aggregation of DNA by Cationic Dendrimers. *Biomacromolecules* **2011**, *12*, 511−517.

(29) Barreleiro, P. C. A.; Lindman, B. The Kinetics of DNA−Cationic Vesicle Complex Formation. *J. Phys. Chem. B* **2003**, *107*, 6208−6213.

(30) Braun, C. S.; Fisher, M. T.; Tomalia, D. A.; Koe, G. S.; Koe, J. G.; Middaugh, C. R. A Stopped-Flow Kinetic Study of the Assembly of Nonviral Gene Delivery Complexes. *Biophys. J.* **2005**, *88*, 4146−4158.

(31) Grueso, E.; Roldan, E.; Sanchez, F. Kinetic Study of the Cetyl Trimethylammonium/DNA Interaction. *J. Phys. Chem. B* **2009**, *113*, 8319−8323.

(32) Wang, R. Y.; Gao, X.; Lu, Y. T. A Kinetic Spectrophotometric Method for Determination of Nitrile by Stopped-Flow Technique. *Anal. Sci.* **2006**, *2*, 299−304.

(33) Wang, R. Y.; Gao, X.; Lu, Y. T. A Surfactant Enhanced Stopped-Flow Kinetic Fluorimetric Method for the Determination of Trace DNA. *Anal. Chim. Acta* **2005**, *538*, 151−158.

(34) Pena, A. M. D. L.; Mansilla, A. E.; Pulgarin, J. A.; Molina, A. A.; Lopez, P. F. Stopped-Flow Determination of Dipyridamole in Pharmaceutical Preparations by Micellar-Stabilized Room Temperature Phosphorescence. *Talanta* **1999**, *48*, 1061−1073.

(35) Wang, R. Y.; Ji, M. N.; Wang, R.; Shi, J. Stopped-Flow Kinetic Fluorimetric Studies of the Interaction of Ru(II) Complex with DNA and its Analytical Application. *Spectrochim. Acta, Part A* **2008**, *71*, 1042−1048.

(36) Porsch, B.; Laga, R.; Horsky, J.; Konak, C.; Ulbrich, K. Molecular Weight and Polydispersity of Calf-Thymus DNA: Static Light-Scattering and Size-Exclusion Chromatography with Dual Detection. *Biomacromolecules* **2009**, *10*, 3148−3150.

(37) Tonomura, B.; Nakatani, H.; Ohnishi, M.; Yamaguchiito, J.; Hiromi, K. Test Reactions for a Stopped-Flow Apparatus—Reduction of 2,6-Dichlorophenolindophenol and Potassium Ferricyanide by L-Ascorbic Acid. *Anal. Biochem.* **1978**, *84*, 370−383.

(38) Braun, C. S.; Vetro, J. A.; Tomalia, D. A.; Koe, G. S.; Koe, J. G.; Middaugh, C. R. Structure Function Relationships of Polyamidoamine/DNA Dendrimers as Gene Delivery Vehicles. *J. Pharm. Sci.* **2005**, *94*, 423−436.

(39) Shah, N.; Steptoe, R. J.; Parekh, H. S. Low-Generation Asymmetric Dendrimers Exhibit Minimal Toxicity and Effectively Complex DNA. *J. Peptide Sci.* **2011**, *17*, 470−478.

(40) Tajarobi, F.; El-Sayed, M.; Rege, B. D.; Polli, J. E.; Ghandehari, H. Transport of Poly Amidoamine Dendrimers Across Madin−Darby Canine Kidney Cells. *Int. J. Pharm.* **2001**, *215*, 263−267.

(41) Chen, C. Y.; Su, C. J.; Peng, S. F.; Chen, H. L.; Sung, H. W. Dendrimer-Induced DNA Bending. *Soft Matter* **2011**, *7*, 61−63.

(42) Eastman, S. J.; Siegel, C.; Tousignant, J.; Smith, A. E.; Cheng, S. H.; Scheule, R. K. Biophysical Characterization of Cationic Lipid: DNA Complexes. *Biochim. Biophys. Acta* **1997**, *1325*, 41−62.
(43) Gershon, H.; Ghirlando, R.; Guttman, S. B.; Minsky, A. Mode of Formation and Structural Features of DNA-Cationic Liposome. *Biochemistry* **1993**, *32*, 7143−7151.
(44) Santhiya, D.; Dias, R. S.; Dutta, S.; Das, P. K.; Miguel, M. G.; Lindman, B.; Maiti, S. Kinetic Studies of Amino Acid-Based Surfactant Binding to DNA. *J. Phys. Chem. B* **2012**, *116*, 5831−5837.
(45) Xu, Q.; Wang, C. H.; Pack, D. W. Polymeric Carriers for Gene Delivery: Chitosan and Poly(amidoamine) Dendrimers. *Curr. Pharm. Des.* **2010**, *16*, 2350−2368.
(46) Sharma, A.; Mohanty, D. K.; Desai, A.; Ali, R. A Simple Polyacrylamide Gel Electrophoresis Procedure for Separation of Polyamidoamine Dendrimers. *Electrophoresis* **2003**, *24*, 2733−2739.
(47) Kukowska-Latallo, J. F.; Bielinska, A. U.; Johnson, J.; Spindler, R.; Tomalia, D. A.; Baker, J. R., Jr. Efficient Transfer of Genetic Material into Mammalian Cells Using. Starburst Polyamidoamine Dendrimers. *Proc. Natl. Acad. Sci. U.S.A.* **1996**, *93*, 4897−4902.
(48) Winnicka, K.; Bielawski, K.; Rusak, M.; Bielawska, A. The Effect of Generation 2 and 3 Poly(amidoamine) Dendrimers on Viability of Human Breast Cancer Cells. *J. Health Sci.* **2009**, *55*, 169−177.
(49) Silva, N. P., Jr.; Menacho, F. P.; Chorilli, M. Dendrimers as Potential Platform in Nanotechnology-Based Drug Delivery Systems. *IOSR J. Pharm.* **2012**, *2*, 23−30.
(50) Ainalem, M. L.; Carnerup, A. M.; Janiak, J.; Alfredsson, V.; Nylander, T.; Schillen, K. Condensing DNA with Poly(amido amine) Dendrimers of Different Generations: Means of Controlling Aggregate Morphology. *Soft Matter* **2009**, *5*, 2310−2320.
(51) Evans, H. M.; Ahmad, A.; Ewert, K.; Pfohl, T.; Martin-Herranz, A.; Bruinsma, R. F.; Safinya, C. R. Structural Polymorphism of DNA−Dendrimer Complexes. *Phys. Rev. Lett.* **2003**, *91*, 75501−75504.
(52) Golan, R.; Pietrasanta, L. I.; Hsieh, W.; Hansma, H. G. DNA Toroids: Stages in Condensation. *Biochemistry* **1999**, *38*, 14069−14076.
(53) Bielinska, A. U.; Chen, C.; Johnson, J.; Baker, J. R., Jr. DNA Complexing with Polyamidoamine Dendrimers: Implications for Transfection. *Bioconjugate Chem.* **1999**, *10*, 843−850.